Heat transfer Model for a Closed Loop Geothermal System: Theoretical Calculation and Experimental Verification

Wei Wang[1], Tingchao Yang[2], Jianshuan Wang[3]*

[1]Hebei Finance University, Baoding, Hebei Province, China
[2]Hydrological geological team of Hebei Province Coal Geology Bureau, Handan, Hebei, China;
[3] Architectural Design and Research Institute, Tianjin University, Tianjin, China
*Corresponding author

Abstract:

As a renewable energy source, geothermal energy (GE) plays an important role in achieving carbon peaking and carbon neutrality. As a form of downhole heat exchanger (DHE), the Closed Loop Geothermal System (CLGS) has the technical characteristics of heat exchange without extracting groundwater, making it a current research hot topic in the utilization of GE. However, there are few theoretical studies on CLGS, and there is a lack of public operating data to verify the practical heat extraction performance of geothermal wells. Based on Piecewise Analytical Solution, this paper established a operating mechanism-based heat transfer model for CLGS. The proposed model solves the problem that the Analytical Solution method lacks consideration of geothermal gradient, and can realize the calculation of fluid distribution in DHE. By comparing the simulated calculation data with the monitoring data in the actual project, it is found that the overall error is less than 3°C, and the average relative error achieves to 7.3%. The research results suggest that the proposed model can provide a simulation verification method for the analysis of the heat transfer characteristics of medium-depth geothermal wells, thereby contributing to the rational utilization of geothermal wells.

Keywords: *Medium-depth geothermal wells; Closed Loop Geothermal System; Coaxial Borehole Heat Exchanger; Analytical Solution method; Geothermal gradient.*

I. INTRODUCTION

With social development and rapid urbanization, the energy demand has increased dramatically [1]. The extensive use of traditional fossil energy has been proven to cause climate warming and ecological degradation [2]. In this case, clean energy, such as solar energy, wind energy and geothermal energy, is considered to be new energy sources that can effectively replace fossil energy in future development scenarios [3-5]. Based on the heat exchange equipment, the ground source heat pump system can use the constant ground temperature throughout the year to cool and heat the interior of the building in summer and winter respectively[6]. In terms of China's geothermal resource endowment and energy policy orientation, ground source heat pump technology has a huge development space due to its low operating

cost and environmental friendliness[7]. The traditional geothermal utilization method directly uses geothermal water for space heating of building, which has relatively high efficiency of heat extraction[8]. However, a large amount of groundwater extraction and poor recharge of water will pollute the surface environment and cause the groundwater level to drop[9]. Therefore, the protective development model of extracting heat without extracting groundwater has become a hot issue in current geothermal energy development[10]. Furthermore, the topics of this research field focus on various forms of downhole heat exchangers, including Coaxial Borehole Heat Exchanger (CBHE)[11], Deep Coaxial Borehole Heat Exchanger (DCBHE) [12], and Closed Loop Geothermal System (CLGS)[13], etc.

Establishing heat transfer mechanism model for CLGS is of great significance for understanding its operating mechanism and improving performance[14]. It is a widely used method to simulate the response of aquifers to geothermal development through numerical models, and analytical solution models are one of the methods that are often used[15]. Furthermore, establishing an accurate heat transfer model for the heat exchanger is the key for design optimization and operation optimization of the system. Horne[16] established a one-dimensional quasi-steady-state heat transfer model for DCBHE, and speculated that the process of heat transfer in the heat storage layer is dominated by heat conduction. In the paper of Rouag, et al.[17], a new transient semi-analytical model was developed to determine the transient change of soil temperature around the pipeline. Through Laplace transform and numerical inversion, Wu, et al.[18] derived a semi-analytical model to analyse the change law of rock and fluid temperature in the process of fluid circulation in the pipeline. By using the convolution theorem, Pan, et al.[19] successfully solved the problem of the temperature rise of the borehole wall and realized high-precision and fast calculation. Luo, et al.[20] introduced the geothermal gradient into the finite line source model, and then developed a segmented finite line system (SFLS) for the quasi-three-dimensional heat transfer in ground well. Wang, et al.[21] used analytical solutions to analyse the one-dimensional radial heat transfer in the backfill material and soil. Moreover, Beier, et al.[22] established an model to simulate vertical temperature curve, providing a new means for evaluating the thermal conductivity under geothermal and thermal resistance of boreholes. Subsequently, Beier, et al.[23] built a model to describe transient heat transfer process and improved their previously proposed model using the Laplace transform method. Furthermore, using balance equation of flow and heat transfer in the soil, Diersch, et al.[24] obtained an effective finite element solution strategy. Mokhtari, et al.[25] optimized the cycle parameters in the coaxial heat exchanger through a genetic algorithm.

As mentioned above, the existing research mainly focuses on the coaxial heat exchanger technology, and relatively rich theoretical research results and field test data have been published. There are only a few related theoretical studies on the deep well heat exchanger technology of closed U-shaped wells. Among the publicly available data, Shaohang, et al. [26] used the method of numerical simulation to analyze the performance of mid-deep U-shaped geothermal wells, and established a heat transfer model inside and outside the pipeline of the heat recovery well on the basis of reasonable assumptions. In its model, the temperature gradient of deep underground rock and soil, lithological changes and the seepage effect of groundwater are mainly considered. Xiaobo[27] analyzed single-well systems and U-shaped geothermal well systems, and established a one-dimensional steady-state heat transfer model for geothermal wells

based on heat transfer theory. The model is suitable for the simulation and analysis of fluid temperature and heat transfer process at any position in the wellbore. Li, et al.[28] developed a three-dimensional full-scale numerical simulation model for the U-shaped geothermal wells on the basis of field experimental data analysis, and verified the model. Based on this model, U-shaped geothermal wells were operated intermittently and continuously. The performance of heat transfer in the pipeline under working conditions was evaluated. Zhou, et al.[29] conducted field experiments on the characteristics of heat transfer in the vertical U-shaped deep buried pipe heat exchange system in the conditions of continuous operation and intermittent operation. They obtained the heat transfer intensity of the buried pipe and the experimental data of geothermal wells of different depths through the temperature difference between the outlet and inlet of the buried pipe, as well as the water flow rate under the experimental conditions. In their paper, it is pointed out that the increase of buried depth has a great influence on heat transfer intensity. Wang, et al. [30] established a vertical U-shaped deep buried pipe heat exchange system with a 2,505m buried depth, and carried out experimental research on characteristics analysis of heat transfer in the conditions of the continuous and intermittent operation of the deep buried pipe system.

In aspect of modeling methods, most existing studies have adopted linear heat sources[31] or column heat source models[32]. The former regards the U-shaped tube as an infinitely long linear heat source of infinite uniform solids, and the latter regards it as a column heat source. However, both of the above models ignore the geometric dimensions of the borehole and assume that the temperature in the thermal reservoir is uniform. Furthermore, the borehole depth of the medium-deep underground heat exchanger is usually 1000~3000m, and the influence of the geothermal gradient is very large, which makes the error of the analytical solution of the line/column heat source very large. The modeling method using numerical simulation technology puts forward a high degree of grid division and time step selection and control when facing the slender geometry of deep buried pipe heat exchanger and complex nonlinear heat transfer process[33]. When the number of grids is too large, the solving calculation will consume a lot of computing resources and time, and it is difficult to apply it to the optimization problem of actual engineering.

Therefore, this paper uses the space segmentation method to establish a set of deep geothermal closed U-tube heat extraction models based on thermodynamic mechanisms. The proposed model can simultaneously simulate the transient changes of the heat exchanger, as well as the surrounding soil temperature, which helps to improve the accuracy and the calculation efficiency of the model. This research can provide a theoretical basis for the subsequent engineering design and system optimization of this article.

II. HEAT TRANSFER MODEL AND ITS ANALYTICAL SOLUTION

2.1 Analysis of heat transfer process

CLGS consists of a pair of wells, which are connected through a link well. During operation, the circulating water is injected from one of the wells, and then flows out through the other well after passing

through the horizontal section, and takes out the underground heat through the metal pipe. Subsequently, the circulating water after the release of heat flows back into the inclined well to obtain heat, and the whole process only takes heat without taking groundwater.

The heat transfer process of CLGS is shown in Fig.1. Specifically, the pipe fluid is forced to convection with the inner wall of the casing by the mechanical force of the water pump, and the inner wall and the outer wall, the outer wall and the backfill material, the backfill material, as well as the soil and rock layer exchange heat in the form of heat conduction.
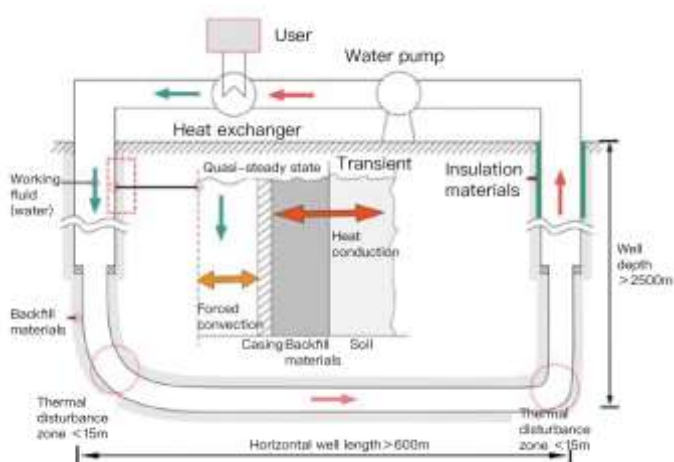

Fig.1: The description of heat transfer mechanism of CLGS

2.2 Basic assumptions about the model

1) For each sub-area, the thermophysical properties of the pipe fluid, the casing and the soil are uniform and isotropic, and do not change with temperature;

2) The soil side is regarded as a pure heat conduction model, and the heat conduction between the sub-regions in the depth direction and the seepage effect of groundwater are ignored;

3) The heat transfer of working fluid in the tube is dominated by convection, while the axial heat transfer process is not considered.

2.3 Simplification of the model

As shown in Fig 2, based on the premise that there is no thermal disturbance between the wells, a three-dimensional closed U-shaped well can be regarded as a two-dimensional model. The boundary condition of each subregion is the initial soil temperature of the corresponding subregion. When the vertical section is divided into n sections, and the horizontal section is divided into m sections, the whole

well produces a total of 2n+m sections. The upper and lower initial temperatures of the two-dimensional model are symmetrical, and the fluid in the tube flows from top to bottom.
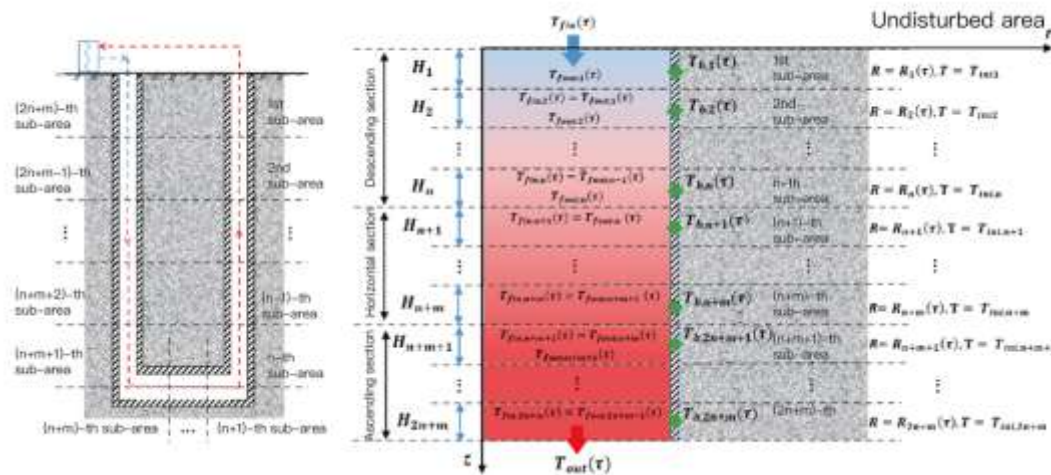

Fig.2: Simplified model established for CLGS

2.4 Model outside the borehole

2.4.1 Determination of the radius of control area

This research introduces the calculation method of thermal influence radius proposed by Wang [34] in the application of energy balance. The specific control equation is as follows:

$$\pi\left(R_2 - r_b^2\right)\left(T_{int} - T_{ini}\right)c_s\rho_s = q_l\tau \tag{1}$$

Where R and r_b denote thermal disturbance radius and the radius of the wellbore, respectively, in m; T_{int} and T_{ini} are the average temperature and initial temperature of the integral median of the soil side, in K; q_l is the heat flux per unit length, in W /m; c_s is the heat capacity of the soil, in kJ/m3·K; ρ_s means the soil density, the unit is kg/m3; τ means the operating time, in s.

In equation (1), the calculation of R requires the operating time (τ) of a given geothermal well, the heat flux density (q_l) transferred through the well wall, the initial soil temperature (T_{ini}), and the integral median of the soil side average temperature (T_{int}). T_{int} is the integral average temperature between the well wall r_b and the thermal disturbance radius R in the soil cylinder. In order to calculate the integrated average temperature, it is necessary to obtain the temperature distribution $T_s(r)$ in the radial direction of the soil first. The soil side temperature distribution $T_s(r)$ and the integrated average temperature T_{int} can be obtained by equations (2) and (3).

$$T_s(r) = T_{ini} - \frac{q_l}{2\pi\lambda_s} \frac{R^2}{R^2 - r_b^2} \left[\ln\left(\frac{r}{R}\right) + \frac{1}{2} - \frac{1}{2}\left(\frac{r}{R}\right)^2 \right] \tag{2}$$

$$T_{int} = \frac{\int_{rb}^{R} 2\pi r T_s(r)\,dr}{\int_{rb}^{R} 2\pi r\,dr} \tag{3}$$

In equations (1)-(3), independent variables include running time (τ), heat flux $q(l)$, initial temperature (T_{ini}) and disturbance radius (R), while the intermediate variable $T_s(r)$ is about heat flux $q(l)$, The relationship between the initial temperature (T_{ini}) and the perturbation radius (R). The above three equations constitute a closed solution, and the mapping relationship between the disturbance radius and other variables is clear. When given the values of known variables and constants, it is easy to find the perturbation radius R through an iterative algorithm.

2.4.2 The model establishment for the outside of borehole

In the heat transfer model of CLGS, the calculation domain is divided into a soil model outside the borehole and a working fluid model inside the borehole. Specifically, the governing equation for the sub-region of the soil model is as follows.

$$\frac{1}{\alpha_s} \frac{\partial T}{\partial \tau} = \frac{1}{r} \frac{\partial}{\partial r}\left(r \frac{\partial T}{\partial r} \right) \tag{4}$$

The corresponding boundary conditions of equation (4) are as follows:

$$q_l = -\lambda_s \frac{\partial T}{\partial r}, r = r_b, \tau > 0 \tag{4-a}$$

$$T_\infty = T_{suf} + \frac{gH}{2}, r = R_i, \tau > 0 \tag{4-b}$$

$$T_{ini} = T_{suf} + \frac{gH}{2}, \tau = 0, r_b < r < R_i \tag{4-c}$$

Where T denotes the soil temperature distribution, which is a function of radial r and time τ; α_s means the soil thermal diffusivity, in m2/s; λ_s is the soil thermal conductivity, in W/m·K; T_{suf} means the surface temperature of the soil, in K (it can be approximated by the average air temperature on the ground); g means the average value of geothermal temperature gradient, in °C/m; H denotes the depth of each sub-region, in m; R_j is the disturbance radius of the j-th sub-region, in m; q_l means the heat flux density, which is the first type of boundary condition in equation (4), in W/m; the position at R_j is the

third boundary condition, and the temperature in the area outside R_j is not disturbed, and the unit is m.

The essence of equation (4) is a homogeneous partial differential equation with non-homogeneous boundary in the cylindrical coordinate system, and the non-homogeneous part of the boundary condition has nothing to do with time. To solve this equation, the inhomogeneous problem can be decomposed into the following two simple problems:

1) A steady-state problem defined by temperature $T_s(r)$;

2) A homogeneous a stable problem defined by $T_h(r, \tau)$.

Since the steady-state problem does not involve time variables, the corresponding $T_s(r)$ can be solved by a simple integral transformation. Subsequently, the separation variable method in the cylindrical coordinate system is used to solve the unsteady-state homogeneous problem of the temperature $T_h(r, \tau)$. Finally, superimpose the two to get the temperature distribution $T(r, \tau)$ in the soil. The specific calculation equations are as follows:

For the defined steady-state problem:

$$
\begin{cases}
T_s(r) = T_{ini} - \dfrac{q_l r_b}{\lambda_s} \ln \dfrac{r}{Ri} \\
T_b(r,\tau) = \sum_{m=1}^{\infty} \dfrac{\pi^2 e^{-\alpha_s \beta_m^2 t}}{2} \dfrac{\beta_m^2 J_1^2(\beta_m, r_b) \left[J_o(\beta_m, r) Y_o(\beta_w, R) - J_o(\beta_w, R) Y_o(\beta_m, r) \right]}{J_1^2(\beta_m, r_b) - J_0^2(\beta_w, R)}
\end{cases}
\tag{5}
$$

$$
\int_{r_b}^{R} \left[J_o(\beta_m, r) Y_o(\beta_w, R) - J_o(\beta_w, R) Y_o(\beta_m, r) \right] F(r) dr
\tag{6}
$$

The equation for the temperature of the soil side at different times and in different radial directions is as follows:

$$
T(r, \tau) = T_s(r) + T_h(r, \tau)
\tag{7}
$$

2.5 Establishment of the model in the borehole

This paper use analytical solution model for the pipe fluid. According to the heat balance equation, the energy equation of the fluid in the sub-region can be described as follows.

$$
-Mc_w \frac{dT_f}{dz} = \frac{T_f(z) - T_{b,j}(\tau)}{R_d}
\tag{8}
$$

Where, the left side of the equation means convective heat transfer generated by fluid flow. The right side of the equation is the heat per unit length that the heat storage transfers to the fluid in the pipe through the wellbore. The schematic diagram can be found in Fig. 2.

The corresponding boundary conditions are as follows:

$$T_f(0) = T_{fin} \qquad (9)$$

Where, M means the fluid volume flow in the tube, in m3/s; c_w menas the heat capacity of water, in kJ/m3·K; $T_f(z)$ meanss the temperature distribution of the fluid in the tube in the z direction, in K; z is the depth , in m; $T_{b,j}(\tau)$ is the wellbore wall temperature at time τ in the j-th sub-region, in K; R_d is the total thermal resistance between inner tube and wellbore wall, in m·K/W; T_{fin} is the sub-region's inlet temperature, in K.

The calculation of x mainly includes three parts, as shown in TABLE I, including the forced convection between the pipe fluid and the casing, the heat conduction between the casing and the heat conduction between the casing and the backfill material. They are represented as x, y, and z in Fig.3. For the closed U-well heat exchanger, considering that the thermal conductivity of the casing and the coefficient of convective heat transfer h under forced convection are relatively large, and the calculated thermal resistance is less than 5% of the thermal resistance of the backfill material; thus it can be ignored.
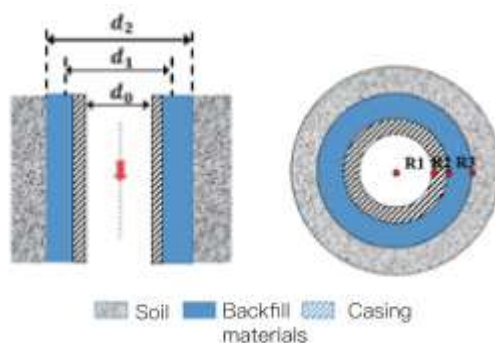

Fig.3: Heat transfer process in the borehole

TABLE I. ANALYSIS OF THE TOTAL THERMAL RESISTANCE COMPOSITION RATIO

THERMAL RESISTANCE COMPOSITION	KEY PARAMETER	THERMAL RESISTANCE (M·K/W)	PERCENTAGE (%)
R_1	$h = 5300$	3.00×10^{-4}	0.7
R_2	$\lambda_g = 46$	4.51×10^{-4}	1.3
R_3	$\lambda_b = 1.5$	4.25×10^{-2}	98

Based on this, the calculation formula for R_d in this study is:

$$R_d = R_3 = \frac{1}{(2\pi\lambda_b)} ln\left(\frac{d_2}{d_1}\right) \tag{10}$$

Among them, d_2, d_1, d_0 represent the wellbore diameter, the outer and inner diameter of the casing, in m. λ_g and λ_b respectively represent the thermal conductivity of the pipe and the thermal conductivity of the backfill material, in W/m·K. h is the convection coefficient between the pipe fluid and the casing, in W/m2·K.

Formula (29) is a simple one-variable differential equation. Through a simple integral transformation, the solution of the governing equation in the tube of the sub-region can be expressed as follows:

$$T_f(z) = \left(T_{fin} - T_b(\tau)\right)e^{-z/R_d Mc_w} + T_b(\tau) \tag{11}$$

Substituting the length Hj of each subregion into z, the outlet temperature of each subregion can be calculated as follows:

$$T_{out} = \left(T_{fin,j} - T_b(\tau)\right)e^{-H_j/R_d Mc_w} + T_b(\tau) \tag{12}$$

Significantly, the outlet temperature for each sub-area is the inlet temperature of the next sub-area, namely T_{fin}.

2.6 Coupling calculation method for the model

As mentioned earlier, the utilization depth of mid-deep geothermal is generally 1000~3000 m, and the bottom temperature of the deep hole can reach 50~100 °C. Therefore, it has to consider the influence of geothermal gradient on the heat transfer of CLGS. In the previous analytical solution models, the initial underground temperature was assumed as uniform. In order to analyze the influence of the inhomogeneity of the geothermal gradient and the dynamic change of the borehole size on the heat transfer process, the calculation area is divided into multiple sub-areas.

In the process of dividing the model, the fluid temperature in the tube and the soil outside the tube in each sub-region is significantly different, resulting in a difference in the corresponding heat flux density of each sub-region. When solving equation (4), q_l needs to be a time-independent value to decompose the second-order partial differential equation into two simpler equations. However, in the actual heat extraction process, q_l will gradually change over time, which is a dynamic parameter. Therefore, it needs to be improved to adapt to the actual situation of q_l changes in the heat transfer process. When introducing the segment into the finite line source model, in order to convert the current solution into a temperature field affected by the dynamic heat source, this paper uses a heat flow processing method, that is, $q_{l,j}$ is equivalent to the effect of the heat flow sequence of heat accumulation, as shown in Fig 4.

$$q_{l,j} = \sum_{j=1}^{Ns}\left(q_{l,j}^{\tau/\Delta\tau-i} - q_{l,j}^{\tau/\Delta\tau-i}\right) \tag{13}$$
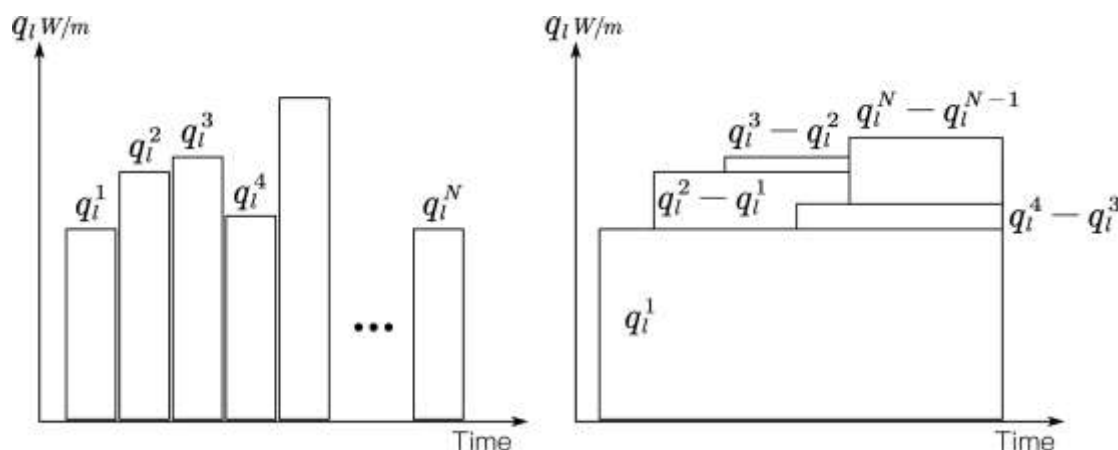

Fig.4: Treatment of equivalent heat flow

Where N_s is the discrete time node. $\Delta\tau$ means the time step (s). τ is the running time.

The calculation formula for the actual heat flux $q_{i,j}(\tau)$ of each sub-model is as follows:

$$q_{l,j}(\tau) = \frac{T_{b,j}(\tau) - T_f(z)}{R_d} \tag{14}$$

The essence of equation (34) is to calculate a series of actual heat flow sequences $q_{l,j}(1)$, $q_{l,j}(2)$, $q_{l,j}(3)$, ... $q_{l,j}(N_s)$ from equation (35) on soil temperature distribution as q_l lasting Ns time to exert heat on the soil. When Ns is 1, $q_l = q_{l,j}(1)$; when Ns is 2, q_l is the composite value of $\left[q_{l,j}(1), q_{l,j}(2)\right]$, and by analogy with rolling operations, the equivalent heat flow $q_{l,j}$ at each time can be calculated. Finally, the equations (1) and (28) can be used to calculate the heat influence radius R and the soil temperature distribution $T(r,\tau)$ at each moment.

It is divided into n sections from top to bottom, and the horizontal section is divided into m sections. After simplifying the entire geothermal well into a two-dimensional model, the model produced a total of 2n+m sub-regions. For each sub-region, the calculation method of the initial soil temperature boundary condition can be calculated by the surface temperature, the depth of the sub-region and the geothermal gradient, as shown in formula (36). Moreover, other piecewise functions can also be used to more accurately describe the difference in geothermal temperature gradients at different depths.

$$\begin{cases} T_{ini,j} = T_{\infty,j} = T_{surf} + \dfrac{gH_j}{2} + \sum_{p=1}^{j-1} gH_p, r = R_j, \tau \geq 0, j = 1, \cdots, n \\[2mm] T_{ini,j} = T_{\infty,j} = T_{surf} + \sum_{p=1}^{n} gH_p, r = R_j, \tau \geq 0, j = n+1, \cdots, n+m \\[2mm] T_{ini,j} = T_{\infty,j} = T_{ini,2n+m-j}, r = R_j, \tau \geq 0, j = n+k+1, \cdots, 2n+m \end{cases} \tag{15}$$

Where $T_{ini,j}$ and $T_{\infty,j}$ respectively represent the initial temperature of the j-th subregion and the soil temperature outside the radius (R) of the disturbance region.

For each sub-area, the temperature of the well wall changes with time as the formula (37):

$$T_{b,j}(\tau) = T_s(r_b, \tau, j), j = 1, \cdots, 2n = m \tag{16}$$

The heat extracted from the ground is the accumulation of the heat flow of each sub-region over time, as follows:

$$Q_S(\tau) = \sum_{j=1}^{j=2n+m} Q_{s,j}(\tau) = q_{l,j}(\tau) \times H_j \times \tau \tag{17}$$

Where $Q_{s,j}(\tau)$ means the heat extraction of the j-th sub-region in the entire calculation cycle, which is also the cumulative value of the heat flow on time scale; $Q_S(\tau)$ is the heat extraction of entire closed U-shaped heat exchanger in the entire calculation cycle.

According to the known inlet temperature of the first sub-region and the initial borehole wall temperature corresponding to the first sub-region, the inlet temperature of the next sub-region and the heat flux density of this sub-region $q_{l,j}(1)$ can be determined. Then, by equation (34), calculate the equivalent heat flow q_l, and then use equations (1), (28), and (37) to determine the wall temperature of the sub-region at the next moment as the boundary condition at the next moment. The inlet temperature of the first sub-area will be used as the inlet temperature of the second sub-area, and the calculation will be repeated. Calculate the fluid temperature distribution in all sub-regions, and combine them to get the temperature distribution of fluid in the tube.

It is worth noting that the number of segments is directly proportional to the length of the model running time. Therefore, it needs to be evaluated according to the characteristics of the model, and reasonable segmentation can ensure accuracy while reducing the model running time.

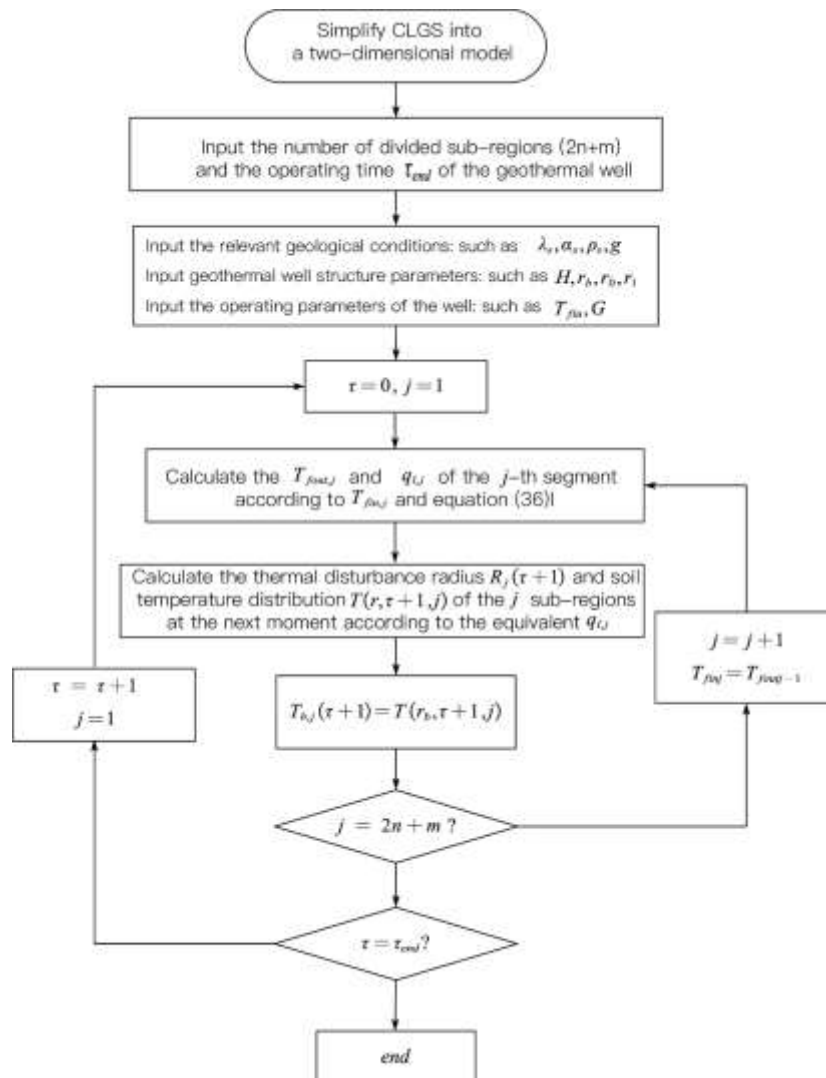The flow of the entire model is shown in Fig. 5.

Fig.5: Flow chart of model coupling calculation method

III. PROJECT EXAMPLE VERIFICATION

3.1. Project introduction

Located in Handan City, Hebei Province, China, the proposed project was completed in 2019, and is responsible for the heating load of 285,000 square meters of buildings and the demand for low-temperature heating at night. As shown in Figure 6, the entire geothermal well is a pair of U-shaped closed geothermal wells with large diameter and long horizontal distance, with a vertical depth of 2500 m and a horizontal spacing of 684 m. The geothermal well device has a metal casing with an outer diameter of 139.7 mm and

an inner diameter of 101.6 mm. The structural parameters and the simulation setting parameters are shown in Fig. 6 and TABLE II.
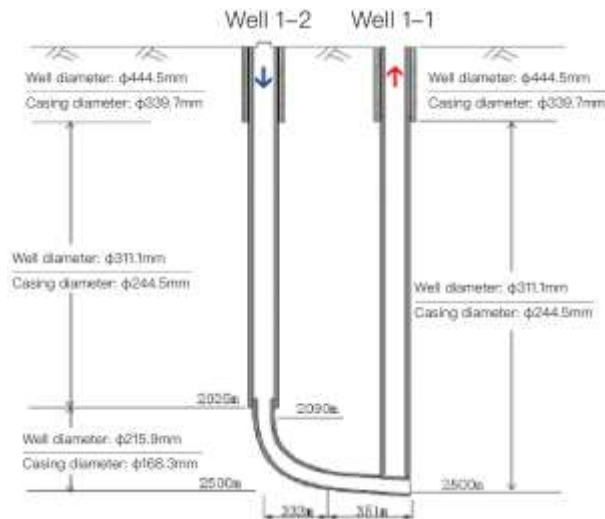

Fig.6: The closed U-shaped well of the proposed project

TABLE II. WELL DEPTH STRUCTURE

WELLS	DRILLING SEQUENCE	WELL DEPTH (M)	CASING SIZE (MM)
STRAIGHT WELL	1	800	444.5/339.7
	2	2500	311.1/244.5
INCLINED WELL	1	800	444.5/339.7
	2	2035	311.1/244.5
	3	2999	215.9/168.3

3.2 Test data

(1) Initial soil temperature

During the geothermal well survey process, well 1-1 was tested and recorded. The test results are shown in Fig 7 and TABLE III.

TABLE III. TEMPERATURE OF THE FORMATION BOUNDARY

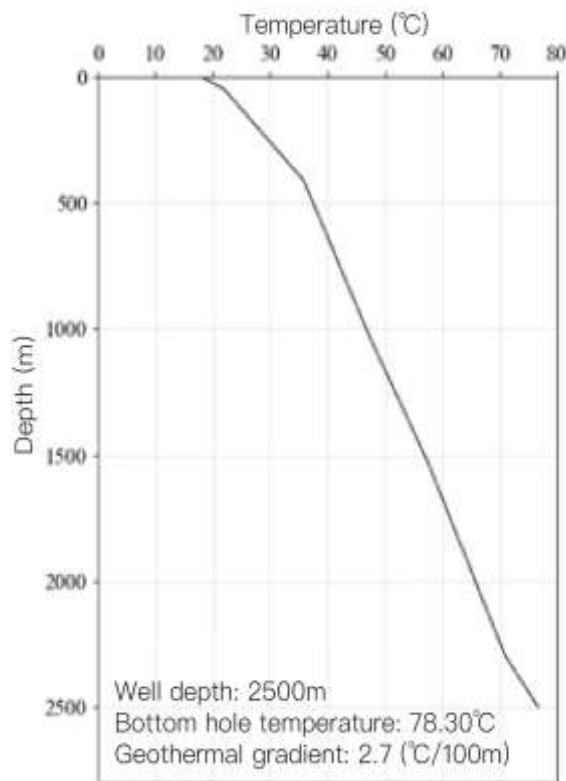| STRATA	DEEPTH(M)	TOP TEMPERATURE (°C)	BOTTOM TEMPERATURE (°C)	TEMPERATURE GRADIENT (°C/100M)
MINGHUA TOWNSHIP FORMATION	413-1030	35.89	47.30	1.85
GUANTAO GROUP	1030-1530	47.30	57.48	2.03
DONGYING FORMATION	1530-2295	57.48	70.90	1.75
SHAHEJIE FORMATION	2295-2500	70.90	76.70	2.82

Fig 7: Initial underground temperature curve

(2) Geological physical parameters

The heat storage types are Minghuazhen Formation, Guantao Formation, Dongying Formation and Shahejie Formation, and the aquifer is thin under the whole geological conditions. Sampling of rock and

soil, some of the sample parameters are described in TABLE IV.

TABLE V. PARAMETERS OF SOIL SAMPLES

SAMPLES	DEPTH	THERMAL CONDUCTIVITY (DRY) (W/M·K)	THERMAL CONDUCTIVITY (WET) (W/M·K)	ROCK DENSITY (G/CM3)	PERMEABILITY (10-3MM2)
MEDIUM SANDSTONE	2439.6~2438.8	2.543	3.309	2.18	234
SILTSTONE	2445.6~2445.8	3.524	3.959	2.57	0.688

Furthermore, the key parameters of the entire geothermal well underground and well structure are shown in TABLE V.

TABLE V. KEY PARAMETER LIST OF SIMULATION SETTING

PARAMETER	UNIT	VALUE	PARAMETER	UNIT	VALUE
WELL DEEP	M	2500	THERMAL CONDUCTIVITY OF BACKFILL MATERIAL	W/(M·K)	1.5
WELL SPACING	M	680	THERMAL CONDUCTIVITY OF PIPE	W/(M·K)	46
WELLBORE DIAMETER	MM	332	SOIL THERMAL CONDUCTIVITY	W/(M·K)	3.5
OUTER PIPE DIAMETER	MM	224	SOIL THERMAL DIFFUSIVITY	M^2/S	1.1×10^{-6}
INNER TUBE DIAMETER	MM	200	GEOTHERMAL GRADIENT	℃/100 M	2.7

3.3 Experimental verification

After the key parameters related to Table 5 and Table 6 were input into the model, simulation calculations were carried out.

TABLE V. INPUT PARAMETER INFORMATION

PARAMETERS	VALUE	UNIT	PARAMETERS	VALUE	UNIT
N	11	SEGMENTS	M	3	SEGMENTS
INLET TEMPERATURE	10	°C	INLET FLOW	90	M^3/H

Insufficient number of divisions of the segmented model will affect the calculation accuracy of the model, and too many divisions, the calculation efficiency of the model will be poor. Considering the balance between model calculation speed and model accuracy, the model is divided into 25 segments after many attempts. Moreover, the central area temperature of each sub-area is taken as average temperature of the entire sub-area to effectively compress the temperature difference caused by the geothermal gradient without causing an excessive burden on the calculation speed. The length of each sub-area is about 200m. A total of 60 days of simulation data were simulated, and the model verification data used 60 days of operating data from November 3 to January 3, 2019. Specifically, 1 to 15 days is the trial operation period, and 16 to 60 days is the official operation period. Figures 8 and 9 show the inlet and outlet temperature and heat output power of a geothermal well, respectively.
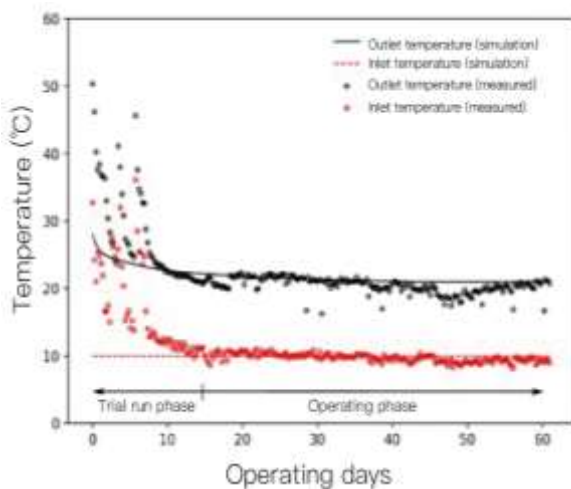

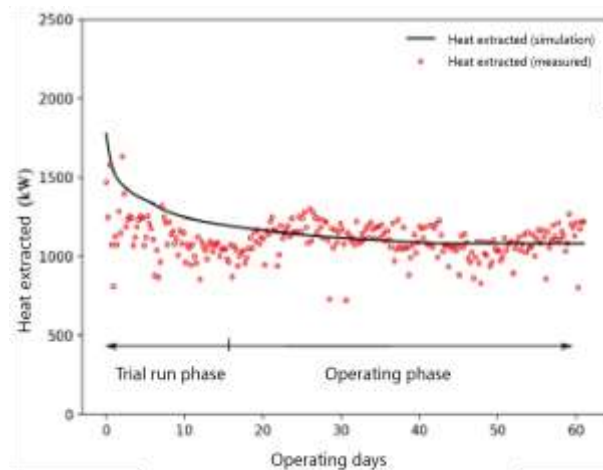Fig. 8: Change of inlet and outlet temperature with operating time   Fig. 9: Variation of output thermal power with operating time

In order to show the results more clearly, select one day's data (such as the 30th day) from the official operation stage for detailed display. Fig. 10 shows the fluid temperature change in the tube along the 30th day under the actual measurement and the fluid temperature in different sub-regions obtained by simulation. Fig.10 shows that the errors between simulated value and measured value mainly appear at 3000~5500m and 0~1000m.

The error at 3000~5500m is due to the use of two optical fibers to monitor different wells respectively. The test data of the optical fiber has a deviation, resulting in a temperature fault at the interface of the two optical fibers. In addition, the fluid temperature at the outlet of the pipe in the ascending well has obvious abnormal fluctuations, so it is believed that the abnormal water temperature change is caused by the second optical fiber signal adjustment error. The error of the first optical fiber sensor between 0 and 1000 m is also relatively large. In fact, under the initial underground temperature field distribution, the underground soil temperature is higher than 10°C, and the inlet fluid temperature in the pipe is set to 10°C. Theoretically, it is impossible for the fluid temperature in the tube to be lower than 10°C along the way, but the actual temperature monitored is 8°C. Therefore, it is determined that the measurement error of the instrument itself or the setting of boundary conditions does not match the actual situation. In addition, the maximum error along the entire geothermal well does not exceed 3°C. The average relative error is 7.3%. It can be considered that the accuracy of the proposed model can meet the engineering requirements.

IV CONCLUSION

Based on theoretical analysis and engineering tests, this research analyzed the heat transfer model for a specific closed U-shaped downhole heat exchanger. By adopting the analytical method of spatial segmentation, the geothermal well is divided into multiple sub-regions, and a model is established for each sub-region. The proposed method effectively solves the problem of insufficient consideration of geothermal gradient in the analytical solution model. By comparing with the operating data of engineering monitoring, it shows that the proposed model can better fit the actual operating conditions. The calculated temperature distribution of the fluid in the heat exchanger tube and the measured data of the optical fiber sensor have a maximum error of less than 3°C along the path, and an average relative error of 7.3%, indicating that the proposed model has good accuracy. The comparative analysis of the heat transfer model and the actual engineering data fills up the research gap in this field. In the future, the proposed calculation tool can be used to further analyze and optimize the design parameters of the closed U-shaped downhole heat exchanger and study its dynamic operating conditions.

ACKNOWLEDGEMENTS

REFERENCES

[1] Marion, J. B., Chapter 1 - THE ENERGY CRISIS. In Energy in Perspective, Marion, J. B., Ed. Academic Press: 1974; pp 1-9.

[2] Lin, B.; Xu, B., How does fossil energy abundance affect China's economic growth and CO2 emissions? Science of the Total Environment 2020, 719, 137503.

[3] Almutairi, K.; Hosseini Dehshiri, S. S.; Hosseini Dehshiri, S. J.; Mostafaeipour, A.; Issakhov, A.; Techato, K., A thorough investigation for development of hydrogen projects from wind energy: A case study. International Journal of Hydrogen Energy 2021, 46, (36), 18795-18815.

[4] Sharif, A.; Meo, M. S.; Chowdhury, M. A. F.; Sohag, K., Role of solar energy in reducing ecological footprints: An empirical analysis. Journal of Cleaner Production 2021, 292, 126028.

[5] Palomo-Torrejón, E.; Colmenar-Santos, A.; Rosales-Asensio, E.; Mur-Pérez, F., Economic and environmental benefits of geothermal energy in industrial processes. Renewable Energy 2021, 174, 134-146.

[6] Eswiasi, A.; Mukhopadhyaya, P., Performance of Conventional and Innovative Single U-Tube Pipe Configuration in Vertical Ground Heat Exchanger (VGHE). Sustainability 2021, 13, (11), 6384.

[7] Zhao, X.-g.; Wan, G., Current situation and prospect of China′s geothermal resources. Renewable and Sustainable Energy Reviews 2014, 32, 651-661.

[8] Zheng, G.; Li, F.; Tian, Z.; Zhu, N.; Li, Q.; Zhu, H., Operation strategy analysis of a geothermal step utilization heating system. Energy 2012, 44, (1), 458-468.

[9] Kong, Y.; Pang, Z.; Shao, H.; Hu, S.; Kolditz, O., Recent studies on hydrothermal systems in China: a review. Geothermal Energy 2014, 2, (1), 19.

[10] Holmberg, H.; Acuña, J.; Næss, E.; Sønju, O. K., Thermal evaluation of coaxial deep borehole heat exchangers. Renewable Energy 2016, 97, 65-76.

[11] Hu, X.; Banks, J.; Wu, L.; Liu, W. V., Numerical modeling of a coaxial borehole heat exchanger to exploit geothermal energy from abandoned petroleum wells in Hinton, Alberta. Renewable Energy 2020, 148, 1110-1123.

[12] Huang, Y.; Zhang, Y.; Xie, Y.; Zhang, Y.; Gao, X., Thermal performance analysis on the composition attributes of deep coaxial borehole heat exchanger for building heating. Energy and Buildings 2020, 221, 110019.

[13] Wang, G.; Song, X.; Shi, Y.; Yulong, F.; Yang, R.; Li, J., Comparison of production characteristics of various coaxial closed-loop geothermal systems. Energy Conversion and Management 2020, 225, 113437.

[14] Wang, G.; Song, X.; Shi, Y.; Yang, R.; Yulong, F.; Zheng, R.; Li, J., Heat extraction analysis of a novel multilateral-well coaxial closed-loop geothermal system. Renewable Energy 2021, 163, 974-986.

[15] Pophillat, W.; Attard, G.; Bayer, P.; Hecht-Méndez, J.; Blum, P., Analytical solutions for predicting thermal plumes of groundwater heat pump systems. Renewable Energy 2020, 147, 2696-2707.

[16] Horne, R. N., Design Considerations of a DownHole Coaxial Geothermal Heat Exchanger. Geothermal Resources Council 1980, 4, 569-572.

[17] Rouag, A.; Benchabane, A.; Mehdid, C.-E., Thermal design of Earth-to-Air Heat Exchanger. Part I a new transient semi-analytical model for determining soil temperature. Journal of Cleaner Production 2018, 182, 538-544.

[18] Wu, B.; Zhang, X.; Jeffrey, R. G., A model for downhole fluid and rock temperature prediction during circulation. Geothermics 2014, 50, 202-212.

[19] Pan, A.; Lu, L.; Cui, P.; Jia, L., A new analytical heat transfer model for deep borehole heat exchangers with coaxial tubes. International Journal of Heat and Mass Transfer 2019, 141, 1056-1065.

[20] Luo, Y.; Guo, H.; Meggers, F.; Zhang, L., Deep coaxial borehole heat exchanger: Analytical modeling and thermal analysis. Energy 2019, 185, 1298-1313.

[21] Wang, C.; Lu, Y.; Chen, L.; Huang, Z.; Fang, H., A semi-analytical model for heat transfer in coaxial borehole heat exchangers. Geothermics 2021, 89, 101952.

[22] Beier, R. A.; Acuña, J.; Mogensen, P.; Palm, B., Borehole resistance and vertical temperature profiles in coaxial borehole heat exchangers. Applied Energy 2013, 102, 665-675.

[23] Beier, R. A.; Acuña, J.; Mogensen, P.; Palm, B., Transient heat transfer in a coaxial borehole heat exchanger. Geothermics 2014, 51, 470-482.

[24] Diersch, H. J. G.; Bauer, D.; Heidemann, W.; Rühaak, W.; Schätzl, P., Finite element modeling of borehole heat exchanger systems: Part 1. Fundamentals. Computers & Geosciences 2011, 37, (8), 1122-1135.

[25] Mokhtari, H.; Hadiannasab, H.; Mostafavi, M.; Ahmadibeni, A.; Shahriari, B., Determination of optimum geothermal Rankine cycle parameters utilizing coaxial heat exchanger. Energy 2016, 102, 260-275.

[26] Shaohang, F.; Jingping, C.; Yanxin, C.; Jinhe, F.; Guoli, F.; Xiaoming, G., Numerical simulation study of the relation between water velocity and heat transfer in the deep geothermal well. Journal of Xi'an University of Architecture & Technology(Natural Science Edition) 2012, 44, (04), 586-592.

[27] Xiaobo, L. Geothermal drilling well type selection and parameter optimization design. Xi'an Shiyou University, Xi'an, 2019.

[28] Li, C.; Guan, Y.; Wang, X.; Li, G.; Zhou, C.; Xun, Y., Experimental and numerical studies on heat transfer characteristics of vertical deep-buried U-bend pipe to supply heat in buildings with geothermal energy. Energy 2018, 142, 689-701.

[29] Zhou, C.; Zhang, Y.; Zhu, Y.; Guan, Y.; Wang, X.; Xun, Y., Innovative vertical U-shaped deep buried pipe heating heat transfer performance experiment. Technology and Innovation Management 2019, 40, (02), 33-37.

[30] Wang, X.; Li, C.; Guan, Y.; Zhou, C.; Xun, Y.; Gui, l., Field experiment of continuous and intermittent operation of building heating with vertical U-shaped deep buried pipe. District Heating 2018, 4, (03), 8-12.

[31] R., I. L., Theory of the ground pipe heat source for the heat pump. Heating Piping and Air Conditioning 1948, 20, 119-122.

[32] D., D. J., Simulation of vertical U-tube ground-coupled heat pump systems using the cylindrical heat source solution. ASHRAE transactions 1991, 97, (01), 287-295.

[33] Li, P. Research on the heat transfer characteristics of the medium-deep geothermal source heat pump casing type underground heat exchanger. Harbin Institute of Technology, Harbin, 2018.

[34] Wang, J., Heat transfer simulations of the buried borehole heat transfer exchangers for engineering applications. In The 10th China International Ground Source Heat Pump Industry Senior Forum, Nanjing, China, 2018.